Journal of Molecular Liquids 386 (2023) 122497

Contents lists available at ScienceDirect

Journal of Molecular Liquids

journal homepage: www.elsevier.com/locate/molliq

A theoretical investigation on the relative stability of the columnar hexagonal and columnar square phases of discotic molecules

Santosh Prasad Gupta [a,*], Mukesh Chandra Bos [a], Shallu Dhingra [b], Santanu Kumar Pal [b,*]

[a] Department of Physics, Patna University, Patna-800005, India
[b] Department of Chemical Sciences, Indian Institute of Science Education and Research (IISER) Mohali, Sector-81, SAS Nagar, Knowledge City, Manauli-140306, India

ARTICLE INFO

Keywords:
Discotic
Square phase
2D hexagonal phase
Order parameter
Mean field theory
Contour plot

ABSTRACT

We have employed a mean field theory, which is a modified Ginzburg-Landau expansion in terms of the scalar order parameter $\Phi(r)$, to stabilize the ordered phases such as square and hexagonal phases of the discotic molecules. The $\Phi(r)$ represents the local volume fraction differential between the stiff core and the outside alkyl chain regions of the discotic molecules. The current theoretical analysis stabilizes the ordered phases, particularly the square (S) and 2D hexagonal (H) phases. The present study also identifies the direct hexagonal (H_I) and reverse hexagonal (H_{II}) phases, with the phases occurring in the following order: $disorder(D)$ - H_I - S - H_{II} - $disorder(D)$ with increase in the average volume fraction difference, Φ_o. Contrarily, the stability area of the S phase accounts for around 10% of the total area of the ordered phase, whereas the H_I and H_{II} phases each occupy about 45% of the total area of the ordered phase.

1. Introduction

One of nature's most efficient methods for creating the dynamic, functional building blocks of life needed to carry out the desired biological activities is molecular self-assembly [1]. Nature uses a variety of supramolecular interactions at various molecular levels to create dynamic functional soft materials, including hydrogen bonding, stacking, polar-non polar interactions, metal coordination, charge-transfer complexes, and ionic interactions. Similar to this, supramolecular systems are fascinating from a scientific standpoint since they mimic the complex natural systems. Liquid crystals (LCs) are the standard for self-organizing molecules in use today among a variety of supramolecular systems. Due to their widespread use in laptops, computers, smart phones, digital cameras, MP3 players, flat-panel TVs, and other electronic devices, LCs can be linked to our daily life. Several angles on LCs have been investigated to reduce the cost, space, energy, raw materials, and to boost the stability and efficiency of these LC materials for easy commercialization [2].

LCs are primarily divided into discotic and rod-like (calamitic) mesogens. The discotic LCs, which Chandrasekhar first identified in 1977, differ from their calamitic counterparts in terms of their molecular structure, phase symmetry, the dimension of their charge transport, exciton migration, and the degree of their orbital overlap [3–7]. The primary building blocks of these discotic systems are rigid aromatic units that are piled on top of one another to create columns that serve as nano-wires. These discotic LCs have extremely high levels of conjugation, which causes the electrons to be substantially delocalized. This results in a smaller band gap, which makes these materials operate as organic semiconductors [8,9].

A typical discotic mesogen has an alkyl side chain that is flexible around a hard, conjugated aromatic core. These discogens form one-dimensional columns by stacking on top of one another through interactions known as 'stacking'. After then, these columns continue to self-organize on different two-dimensional (2D) lattices like hexagonal, rectangular, square, etc.

The four basic types of mesophase produced by discotic mesogens are the nematic, smectic, columnar, and cubic phases [10–13]. A comparable orientational order to that seen in nematic phases of calamitic LCs is present in the nematic phase of discotic LCs, also known as the discotic nematic (N_D) mesophase. Moreover, discotic mesogens have the ability to stack themselves into short columns that are arranged in their orientation rather than in a two-dimensional positional manner. This indicates that short-range positional order and long-range orientational order are characteristics of discogens in this type of self-assembly. Nematic columnar (N_{Col}) mesophase is the word used to describe these phases.

* Corresponding authors.
E-mail addresses: santosh-phy@patnauniversity.ac.in, drspgpu@gmail.com (S.P. Gupta), skpal@iisermohali.ac.in, santanupal.20@gmail.com (S.K. Pal).

https://doi.org/10.1016/j.molliq.2023.122497
Received 19 April 2023; Received in revised form 25 June 2023; Accepted 30 June 2023
Available online 4 July 2023

These discotic units can also exhibit smectic phases. Although the molecules do not form any columnar aggregates during the discotic smectic phase, the discs are stacked in layers that are divided by sublayers of peripheral chains [10].

Interestingly, the columnar mesophase is the most frequently observed type of mesophase created by discotic LCs. This is further supported by the fact that discogens mostly comprise conjugated units, which prefer to organize into columns as a result of interactions between the discotic units. Different 2D lattices created by one-dimensional columns serve as the basis for differentiating columnar mesophases. The degree of order in the molecular stacking, the orientation of the molecules along the columnar axis, the dynamics of the molecules within the columns, and other variables all play a role in how these varied 2D lattices arise. These columnar LCs can be broadly divided into seven groups, including (i) columnar hexagonal, (ii) columnar rectangular, (iii) columnar oblique, (iv) columnar plastic, (v) columnar helical, and (vi) columnar square (tetragonal) and (vii) columnar lamellar mesophases [10,11,13].

Columns are arranged on a 2D hexagonal lattice in the columnar hexagonal (Col_h) phase. The constituent discs inside the columns can be ordered or disordered, which is reflected in the various values of their correlation lengths. When columns are slanted with respect to the columnar axis, as is the case with columnar rectangular (Col_r) mesophase, the result is an elliptical cross-section of the columns. On a rectangular lattice, these columns are placed. Although the cores of a column should be tilted with regard to the cores of neighboring columns, strong core-core interactions are necessary for the creation of the Col_r phase. Similar to the Col_r phase, the constituent columns of the columnar oblique (Col_{ob}) mesophase are arranged on a 2D oblique lattice. A three-dimensional arrangement in any of the above-mentioned columnar lattices makes up the bulk of the columnar plastic (Col_p) phase. The motional freedom of the discs, which is normally observed in the aforementioned columnar phases, is restricted in the Col_p phase and is only permitted to rotate along the columnar axis. Columnar square or tetragonal (Col_{tet}) represents the mesophase where columns are upright and organized on a square lattice. This mesogen exhibit simple homeotropic alignment of columns. Columns made up of stacked discotic mesogens are grouped in layers in columnar lamellar (Col_L) mesophase. There is no spatial association between the columns of various levels, and layers' columns are free to slide. Cubic phase is the final mesophase variant shown by discotic LCs. In the cubic phase, discotic mesogens are arranged in branched, interlaced columns that form a cubic lattice. In discotic LCs, this phase is seldom ever seen.

Instead of the discotic molecule system, there are other systems that are known to display various kinds of self-assembled structures, including amphiphile-water systems and di-block copolymers. To comprehend the intriguing phase behavior of amphiphile-water systems, several theories and methodologies have been used [14–16]. By connecting the (local) molecular form of the aggregating amphiphilic molecules to the (global) composition of the amphiphile-water combination, S. T. Hyde estimated the phase diagram in this relationship. Except for the classical phases, the theory was able to stabilize the cubic, tetragonal, and rhombohedral phases [14,15]. Using a similar strategy, research on the conflict between hydrocarbon chain packing factors and monolayer elastic curvature has provided significant insight into the mesomorphic behavior of lipid-water systems [16]. The morphology chosen by diblock copolymers self-assemblies has also been the subject of several theoretical research [17–19]. In this regard, Matsen computed the binary phase diagrams of the homopolymer A and the diblock copolymer AB, both of which had comparable levels of polymerization [17,18]. This theoretical study shows that different phases coexist amid the ordered mesophases and is based on a self-consistent field theory. Masten and Bates also give a mean-field phase diagram for conformationally symmetric diblock melts using the conventional Gaussian polymer model. The theory stabilizes the many types of cubic phases as well as lamellar structure, and it spans the weak- to strong-segregation regimes without the need of conventional approximation [19].

The mesophases of the discotic molecules have been studied using a variety of mean field models [20,21]. The theory proposed a phase transition from rectangular columnar to hexagonal columnar, assuming that molecules are bi-axial in both phases. The resulting phase sequence predicted by the theory is rectangular, hexagonal, nematic, and isotropic [20]. Additionally, several molecular tilt-induced transitions from phases with hexagonal to those with lesser symmetry were described. There are certain orientational features that are expected and others that are explained [21]. The phase behavior of discotic molecules interacting via a Gay-Berne potential has been studied using a density-functional theory. This has led to the study of the isotropic-nematic-columnar phase behavior for different aspect ratios of the discotic molecules [22].

In the present study, a modified Ginzburg-Landau theory has been used to examine the stability of the discotic molecule-based 2D hexagonal and square phases. The stability of the 2D hexagonal and square phases could be equivalent to the columnar hexagonal and columnar square phase of the discotic by assuming that the length of columns of discotic molecules are very long in comparison to that of the diameter of the discotic molecule and also assuming that the interactions between the discotic core and core and the alkyl chain and chain are strong in comparison to the interactions between the discotic core and alkyl chain. For the columnar square and columnar hexagonal phases, respectively, we have used the S and H symbols here and moving forward. The discotic columns are set up in these phases on 2D square and hexagonal lattices, respectively. The corresponding order parameter, $\Phi(r)$ is expanded in terms of reciprocal lattice vectors corresponding to the first shell of these phases in their corresponding reciprocal lattices. Additionally, it is discovered that this theoretical approach stabilizes the hexagonal and square phases.

The structure of the current article is described below. The following part introduces the Ginzburg-Landau free energy functional of a single order parameter, which is used throughout this paper. In section 3, free energy curves for the H and S phases that vary with respect to average volume fraction difference, Φ_o for various values of the parameters A and B, are calculated once the order parameter has been established. The estimated equilibrium phase diagram was also presented in the A-Φ_o plane. Section 4 marks the conclusion of this article.

2. Theory

We are aware that simple liquid mixtures frequently undergo macrophase separation under specific circumstances. But systems containing two different-property components, including block copolymers, surfactants, discotic molecules, etc., go through microphase separation at low temperatures. Regularly organized ordered structures, such as lamellar, hexagonal, body-centered-cubic (BCC), columnar hexagonal, columnar square, columnar rectangular, and gyroid phases, are typical of microphase separation formations. In this work, we concentrated on the stability of the discotic molecules' mesophases.

The key components of discotic LCs are a central core with a conjugated disc shape that encourages the crystalline character and periphery flexible alkyl chains that make it easier for the liquid character to exist. By altering the size, form, and composition of the central discotic core as well as the type of flexible side chains, it is possible to create discotic LCs with various mesophase morphologies. Or, to put it another way, the discotic molecule can be thought of as a mixture of a rigid core region surrounded by a flexible alkyl chain regime, where the relative volume fraction of these two regimes controls the mesophase morphologies.

To build a Ginzburg-Landau model for the self-assembly of discotic molecules, one must first choose which degrees of freedom in the system are deemed to be crucial and must therefore be included in the model. Let's assume that discotic core-core interactions and alkyl chain-chain

contacts are both quite strong, but discotic core-alkyl chain interactions are weak. Thus, for the theoretical calculations, the local density differential between the two components, the rigid core and the outside alkyl chains regions of the discotic molecules, could potentially be used as the scalar order parameter field, $\Phi(r)$. These two elements may be seen as two regular fluids for the intent of theoretical calculations, and the system of discotic molecules can be seen as a binary fluid mixing of these two regular fluids with isotropic interactions between them. Imposing the incomprehensibility condition $\Phi_{chain}(r) + \Phi_{core}(r) = 1$, where $\Phi_{chain}(r)$ is the local volume fraction of the alkyl chain component and $\Phi_{core}(r)$ is the local volume fraction of the core part of the discotic molecule system, the free-energy functional can be written in terms of the local volume fraction difference, $\Phi(r) = \Phi_{core}(r) - \Phi_{chain}(r)$ as:

$$F = \frac{\int f(\Phi(r))dr}{\int dr} \tag{1}$$

Where $f(\Phi(r)) = A\Phi^2(r) + B\Phi^4(r)$

The free energy density (local) of the homogeneous order parameter, $\Phi(r)$, is expressed as $f(\Phi(r))$. Additionally, the parameters A & B comprise interactions like core-core, core-alkyl chain, chain-chain, column-column, etc. in addition to shape-driven interactions, etc. As a result, these parameters, A & B, depend on factors like pressure and temperature. By integrating $f(\Phi(r))$ over the ordered phase's unit cell and then dividing the result by the cell's size, one can obtain the averaged free energy density, F (global). As a result, the unit of F and the unit of free energy density $f(\Phi(r))$ are the same. Although the free energy is relatively easy to work with, it does not contain terms like molecular orientations and many others. The similar free energy has also been utilized to explain a variety of systems, including magnetic layers [23], Langmuir films [24], diblock copolymers [25], and micro-emulsions [26]. The theory demonstrated the changeover between the stripe and bubble (hexagonal) phases in relation to the magnetic layers [23]. The investigation of the impact of dipolar interactions in Langmuir monolayers in the context of Langmuir films has been discussed by D. Andelman et al. Their primary impact is the stabilization of super-crystal phases whose in-plane concentration oscillates [24]. The idea behind di-block copolymers' ability to display a range of mesophases [25]. G. Gompper et al. demonstrated using a Ginzburg-Landau free energy that a microemulsion's ability to wet an oil/water interface is directly connected to the structure of the microemulsion. Additionally, they demonstrated using a lattice model that when a microemulsion coexists with an incipient lamellar phase instability, the interfacial tensions between oil and water are extremely low [26]. Moreover, this free energy function is quite general and has no bearing on any particular system.

3. Results and discussion

3.1. Order parameter for different phases

In our model, ordered phases can become stable if the core-core and alkyl chain-chain interactions are stronger than the core-alkyl chain interaction, which permits a strong segregation. Here, we write the ordered phase configurations and keep looking for arrangements that minimized the free energy density functional, F (Eq. (1)). The order parameter field, $\Phi(r)$, is extended in a Fourier series as

$$\Phi(r) = \Phi_o + \sum_{i=1}^{i=N} \sum_{G\ \epsilon\ S_i} \Phi_G(r)\ Cos(\vec{G}.\vec{r}) \tag{2}$$

$\Phi(r)$ is made up of the modulated term and the constant term, Φ_o. Further, the Φ_o is the average volume fraction difference, because, the average value of the $\Phi(r)$ across the phase's unit cell equals Φ_o. In the modulated term, $\vec{G}$ stands for the reciprocal vectors, and $\Phi_G(r)$ is the corresponding Fourier or scattering amplitude. S_i signifies the i^{th} cell of the reciprocal vectors. We have, however, only employed the reciprocal vectors that are associated with the first cell of the reciprocal lattice of the ordered phases. Our current research focuses on comparing the stability of the columnar square (S) and hexagonal (H) phases, which create square and hexagonal lattices, respectively, in their two-dimensional projections. Nonetheless, the disorder phase (D) is also included in our study for reference. It should be emphasized that we haven't considered any interactions between the columns of the columnar phases of the discotic molecules other than assuming that there are stronger interactions between the discotic core and core and between the alkyl chain and chain than there are between the discotic core and chain. Also, it is necessary to note that the electron density of the core region is higher than that of the alkyl chain portion. The fact that this theoretical formalism cannot be directly compared to the actual system must also be kept in mind.

For the D, S, and H phases, let's designate the scalar order parameter as $\Phi_D(r)$, $\Phi_S(r)$, & $\Phi_H(r)$, respectively. In the disorder phase, the modulated portion of the order parameter is zero because, as implied by the phase's name, the value of the order parameter is roughly constant throughout the unit cell. Because there is just one Φ_o term in the $\Phi_D(r)$, the expression for the $\Phi_D(r)$ can be written as follows:

$$\Phi_D(r) = \Phi_o \tag{3}$$

In the case of the S phase, let's assume that the lattice parameter is a_s. Thereafter, direct basis vectors can be expressed as:

$$\vec{a} = a_s\hat{i} \quad \& \quad \vec{b} = a_s\hat{j} \tag{4}$$

resulting in the reciprocal basis vectors being:

$$\vec{a^*} = \frac{2\pi}{a_s}\hat{i} \quad \& \quad \vec{b^*} = \frac{2\pi}{a_s}\hat{j} \tag{5}$$

As is well known, the reciprocal lattice vector is represented by:

$$\vec{G} = h\vec{a^*} + k\vec{b^*} \tag{6}$$

Hence, after accounting for the values of a^* and b^* in the relationship above, we have

$$\vec{G} = \frac{2\pi}{a_s}[h\hat{i} + k\hat{j}] \tag{7}$$

Where h and k are the Miller indices of the reflecting planes of square lattice. As a result, the reciprocal lattice vectors in the first cell of the reciprocal lattice corresponding to square lattice are as follows (Fig. 1[i] & [ii]):

$$\vec{G}_{10} = \frac{2\pi}{a_s}\hat{i},\ \ \vec{G}_{\bar{1}0} = -\frac{2\pi}{a_s}\hat{i},\ \ \vec{G}_{01} = \frac{2\pi}{a_s}\hat{j},\ \ \vec{G}_{0\bar{1}} = -\frac{2\pi}{a_s}\hat{j} \tag{8}$$

Thus, the formulation of the $\Phi_S(r)$ in line with Eq. (2) can be expressed as follows:

$$\Phi_S(r) = \Phi_o + A_S\ [Cos(\frac{2\pi x}{a_s}) + Cos(\frac{2\pi y}{a_s})] \tag{9}$$

Where, A_S is the scattering (Fourier) amplitude corresponding to the square lattice.

Similar to this, let's assume that the lattice parameter in the hexagonal phase is a_h. Direct basis vectors are then represented as:

$$\vec{a} = a_h\hat{i} \quad \& \quad \vec{b} = -\frac{a_h}{2}\hat{i} + \frac{\sqrt{3}\,a_h}{2}\hat{j} \tag{10}$$

as a result, the reciprocal basis vectors are:

$$\vec{a^*} = \frac{2\pi}{a_h}(\hat{i} + \frac{\hat{j}}{\sqrt{3}}) \quad \& \quad \vec{b^*} = \frac{4\pi}{a_h\sqrt{3}}\hat{j} \tag{11}$$

Hence, after taking into account the values of a^* and b^*, we have

$$\vec{G} = \frac{2\pi}{a_h}[h\hat{i} + (\frac{h}{\sqrt{3}} + \frac{2k}{\sqrt{3}})\hat{j}] \tag{12}$$

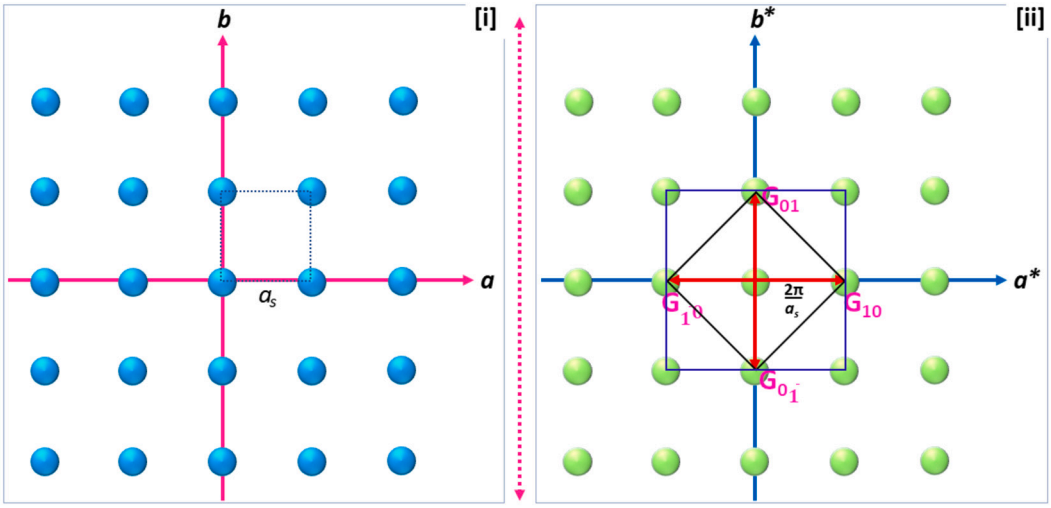

Fig. 1. [i] showing the direct square lattice where a_s is the lattice parameter. [ii] Reciprocal lattice corresponding to the square lattice. Rhombus in black color denotes the first cell and square in blue color represents the second cell in the reciprocal space. The red colored vectors ($\vec{G}_{10}, \vec{G}_{\bar{1}0}, \vec{G}_{01}$&$\vec{G}_{0\bar{1}}$) correspond to the reciprocal vectors in the first cell.

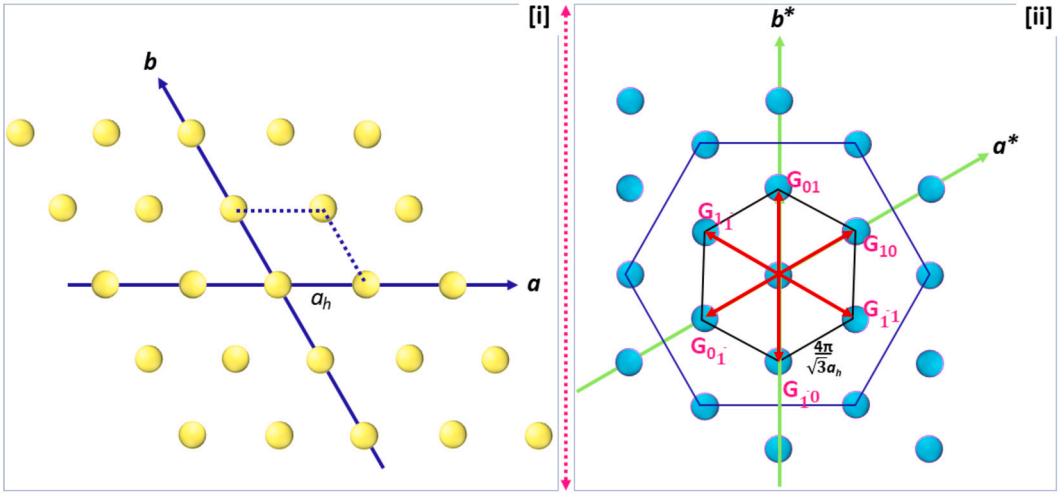

Fig. 2. [i] Display direct 2D hexagonal lattice where a_h is the lattice parameter. [ii] shows a lattice that is reciprocal to the hexagonal lattice. In the reciprocal space, the first cell is represented by a hexagon in black color, while the second cell is shown by a hexagon in blue color that has been rotated by 30 degrees with respect to the first one. The vectors $\vec{G}_{10}, \vec{G}_{\bar{1}0}, \vec{G}_{01}, \vec{G}_{0\bar{1}}, \vec{G}_{1\bar{1}}$ & $\vec{G}_{\bar{1}1}$ in red color correspond to the reciprocal vectors in the first cell.

As a result, the reciprocal lattice vectors in the first cell of the reciprocal lattice that corresponds to the two-dimensional hexagonal lattice are as follows (Fig. 2[i] & [ii]):

$$\vec{G}_{10} = \frac{2\pi}{a_h}(\hat{i} + \frac{\hat{j}}{\sqrt{3}}),\quad \vec{G}_{\bar{1}0} = -\frac{2\pi}{a_h}(\hat{i} + \frac{\hat{j}}{\sqrt{3}}),\quad \vec{G}_{01} = \frac{4\pi}{a_h\sqrt{3}}\hat{j},$$
$$\vec{G}_{0\bar{1}} = -\frac{4\pi}{a_h\sqrt{3}}\hat{j}, \vec{G}_{1\bar{1}} = \frac{2\pi}{a_h}(\hat{i} - \frac{\hat{j}}{\sqrt{3}}),\quad \vec{G}_{\bar{1}1} = -\frac{2\pi}{a_h}(\hat{i} - \frac{\hat{j}}{\sqrt{3}}) \tag{13}$$

so that the expression for $\Phi_H(r)$ in line with Eq. (2) can be expressed as follows:

$$\Phi_H(r) = \Phi_o + A_H\ [Cos\frac{2\pi}{a_h}(x + \frac{y}{\sqrt{3}}) + Cos\frac{4\pi}{a_h}(\frac{y}{\sqrt{3}}) + Cos\frac{2\pi}{a_h}(x - \frac{y}{\sqrt{3}})] \tag{14}$$

Where, A_H is the scattering (Fourier) amplitude corresponding to the two-dimensional hexagonal lattice.

3.2. Free energy for different phases

Combining the three equations (3), (9), (14) we obtain

$$\Phi_D(r) = \Phi_o \tag{15a}$$
$$\Phi_S(r) = \Phi_o + A_S\ [Cos(\frac{2\pi x}{a_s}) + Cos(\frac{2\pi y}{a_s})] \tag{15b}$$
$$\Phi_H(r) = \Phi_o + A_H\ [Cos\frac{2\pi}{a_h}(x + \frac{y}{\sqrt{3}}) + Cos\frac{4\pi}{a_h}(\frac{y}{\sqrt{3}}) + Cos\frac{2\pi}{a_h}(x - \frac{y}{\sqrt{3}})] \tag{15c}$$

By substituting the $\Phi(r)'s$ of the phases from equation (15) into equation (1), the expression of free energy density (F) of the aforementioned phases is derived. Let's use the symbols F_D, F_S, and F_H to designate free energy density of the D, S, and H phases, respectively. Then we have

$$F_D(A, B, \Phi_o) = A\ \Phi_o^2 + B\ \Phi_o^4 \tag{16a}$$
$$F_H(A, B, \Phi_o) = A\ \Phi_o^2 + B\ \Phi_o^4 + \frac{3}{8}\ A_H^2\ (4A + B(15\ A_H^2\ \Phi_o + 16\ A_H + 24\ \Phi_o^2)) \tag{16b}$$

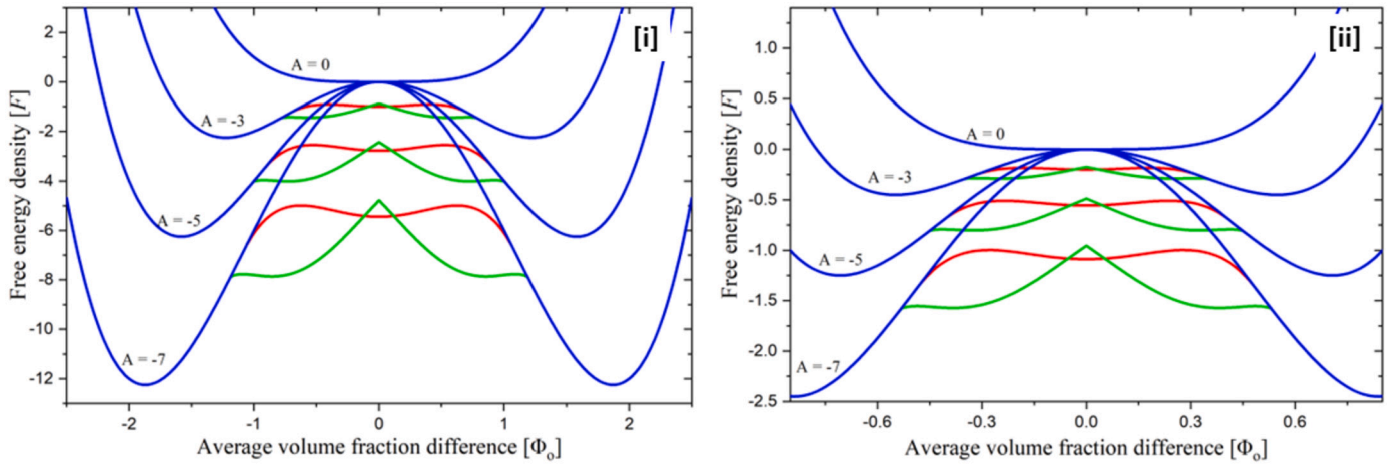

Fig. 3. Variation of free energy density (F) for the square (S), Hexagonal (H) and disorder (D) phases with respect to average volume fraction difference (Φ_o) at the value of parameter [i] $B = 1$ and [ii] $B = 5$. For each value of B the value of parameter: $A = 0, -3, -5, -7$, curve in red, green, & blue colors correspond to square (S), hexagonal (H) and disorder (D) phases, respectively.

$$F_S(A, B, \Phi_o) = A\,\Phi_o^2 + B\,\Phi_o^4 + A\,A_S^2 + \frac{1}{4}(9B\,A_S^4) + 6B\,A_S^2\,\Phi_o^2 \qquad (16c)$$

Each phase's free energy density has four variational parameters, A, B, Φ_o, and the scattering (Fourier) amplitude. Free energy density is minimized with regard to the Fourier amplitude of each phase for each combination of A, B, and Φ_o. And for that set of variational characteristics, the phase with the lowest energy is stable.

3.3. Free energy curves

Fig. 3 depicts the variations in the free energy density (F) of the various phases with regard to Φ_o at various values of A & B. In this case, the free energy was estimated for $B = 1$ and $B = 5$, and the value of A was set at $0, -0.5, -1, -3, -5$, and -7 for each value of B.

According to Fig. 3, the free energy density variation with respect to Φ_o in the case of the S phase contains minima at $\Phi_o = 0$ and two additional minima symmetrically positioned about $\Phi_o = 0$, one at the positive side and one at the negative side of Φ_o. As seen in the figure, the value of the free energy corresponding to these minima rises as A increases, while the distance between the two symmetrical minima reduces and eventually combines to form the minima at $\Phi_o = 0$. The free energy curve for the H phase, on the other hand, contains two deep minima that are symmetrically located near $\Phi_o = 0$ and on each side of $\Phi_o = 0$ and a cusp at $\Phi_o = 0$. The value of the free energy density corresponding to these minima and cusp grows as A is increased in value. However, as seen in the images (Fig. 3), the minimum and cusp were ultimately discovered to be merging and changing into a minima at $\Phi_o = 0$. Moreover, the disorder phase's free energy density curve features two symmetric minima located around $\Phi_o = 0$ and maxima at $\Phi_o = 0$. As the value of A rises, so does the value of the free energy density corresponding to these peaks and minima. Yet, at $\Phi_o = 0$, these minima and maxima transform into a minima, as seen in Fig. 3. Moreover, for $B = 5$, the shape of the free energy density curves for the S, H and D phases is identical to that at $B = 1$. Yet, it is discovered that the stability range of the ordered phases (H, & S) in the Φ_o is smaller at $B = 5$ than it is at $B = 1$.

3.4. Phase diagram : Φ_o - A plane

The diagrams (Fig. 3) make it evident that the S phase has the lowest free energy density among all the phases at and very close to $\Phi_o = 0$. Additionally, the H phase is stable when one moves away from $\Phi_o = 0$ on either side. Nevertheless, all of these free energy curves eventually combine to form the D phase either by departing from $\Phi_o = 0$ very far or by raising the value of A for each increase in B. As a result of the findings made above, it can be said that on either side of the point where $\Phi_o = 0$, the initial S phase stabilizes, followed by the H phase, and then the D phase eventually takes control. The stability area of the ordered phases, S, H, in the Φ_o - A plane of the phase diagram also declines with rising A value and eventually becomes zero at $A = 0$. As a result, the D phase entirely took control of the orderly phase at $A = 0$. Yet, behavior at $B = 5$ is quite similar to that at $B = 1$, although the ordered phase's stability zone in the Φ_o - A plane is shorter. From the free energy density curves for different values of A and for $B = 1$ and $B = 5$, the (Φ_o, A) coordinates of the $S - H$ and $H - D$ phase boundaries have been computed, and they are listed in Table 1, respectively. Plotting these coordinates as A against Φ_o yields the phase diagram (Fig. 4).

Table 1
(Φ_o, A) coordinates corresponding to the phase boundaries; Square-Hexagonal, & Hexagonal-Disorder with accuracy in Φ_o is ±0.0002 at $B = 1$ and $B = 5$.

$B = 1$				$B = 5$			
Square-Hexagonal		Hexagonal-Disorder		Square-Hexagonal		Hexagonal-Disorder	
Φ_o	A	Φ_o	A	Φ_o	A	Φ_o	A
-0.1178	-7	-1.1901	-7	-0.0527	-7	-0.5400	-7
-0.0996	-5	-1.0100	-5	-0.0444	-5	-0.4500	-5
-0.0771	-3	-0.7801	-3	-0.0344	-3	-0.3501	-3
-0.0444	-1	-0.4520	-1	-0.0199	-1	-0.2100	-1
-0.0252	-0.5	-0.3200	-0.5	-0.0113	-0.5	-0.1500	-0.5
0	0	0	0	0	0	0	0
0.0252	-0.5	0.3200	-0.5	0.0113	-0.5	0.1500	-0.5
0.0444	-1	0.4520	-1	0.0199	-1	0.2100	-1
0.0771	-3	0.7801	-3	0.0344	-3	0.3501	-3
0.0996	-5	1.0100	-5	0.0444	-5	0.4500	-5
0.1178	-7	1.1901	-7	0.0527	-7	0.5400	-7

In order to comprehend the nature of these ordered phases, H & S, related scattering amplitudes, A_H & A_S, have been calculated at $A = -7$, $B = 1$ & at $A = -7$, $B = 5$ and at various values of Φ_o included in these phase region (Fig. 5[i]). The calculated value of scattering amplitude, A_H for the H phase is discovered to be positive for the negative value of Φ_o. Including the value of A_H into $\Phi_H(r)$ and creating the matching contour plot afterwards results in a pattern where the only region that may display the 2D hexagonal lattice is one with the highest electron density (Fig. 5[i] & 6[i]). This is the columns of core distributed in the matrix of the alkyl chain on the hexagonal lattice; as a result, the phase is direct hexagonal and is represented by the symbol H_I. For instance, Fig. 6[i] displays the contour plot of $\Phi_H(r)$ at $A = -7$, $B = 1$, and $\Phi_o = -0.5$ with an optimal value of $A_H = 1.07939$. In the H phase region, it is also discovered that the value of A_H is negative for the

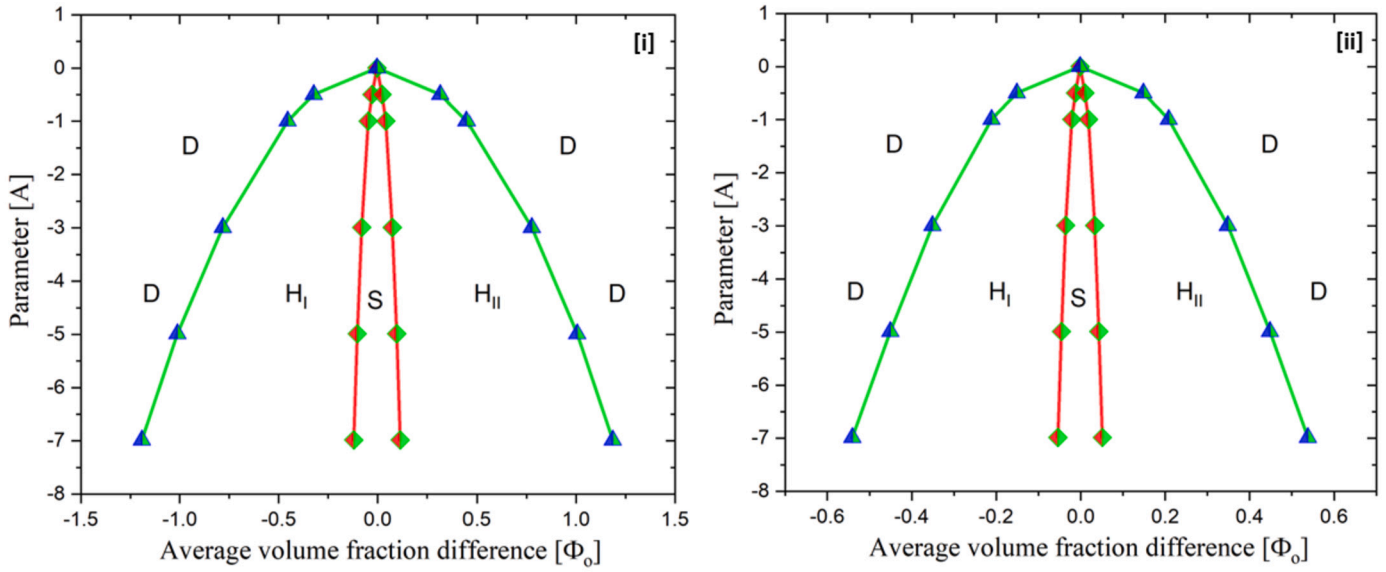

Fig. 4. Phase diagram in the $A-\Phi_o$ plane at [i] $B=1$ and [ii] $B=5$. S, H_I, H_{II} and D correspond to square, hexagonal (direct), hexagonal (inverse), and disorder phases, respectively.

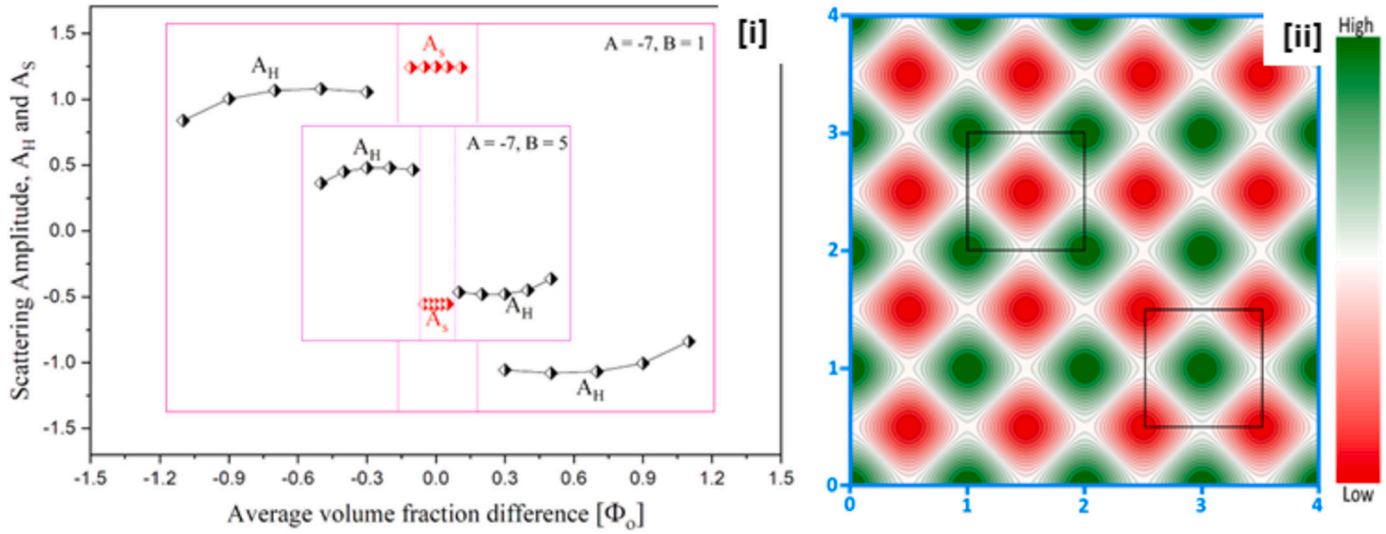

Fig. 5. [i] Showing the variation in the scattering (Fourier) amplitudes A_H and A_S in relation to Φ_o in their respective phases. The purple box in inset is associated with parameter $A=-7$ & $B=5$, while the red box in the inset is related to parameter $A=-7$ & $B=1$. The scattering amplitude, A_H, is represented by the half-filled diamond in black, and the scattering amplitude, A_S, by the half-filled diamond in red. [ii] Contour plot of $\Phi_S(r)$ at $A=-7$, $B=1$, and $\Phi_o=-0.05$ with optimal value of $A_S=1.24588$; deep red hue corresponds to highest electron density, and deep green is the lowest. Scale is given in the unit of the lattice parameter. The square lattice's unit cell is represented by a square. The square lattice can be found in regions with low electron densities as well as with the high electron densities.

positive value of Φ_o. After adding the A_H value, the accompanying contour plot of $\Phi_H(r)$ displays a pattern where only the regions with the lowest electron density may exhibit the 2D hexagonal lattice. The phase is reverse hexagonal and is indicated by the symbol H_{II} since this is the columns of alkyl chains distributed on the hexagonal lattice in the core matrix. Fig. 6[ii] provides an illustration of the contour plot of $\Phi_H(r)$ at $A=-7$, $B=1$, and $\Phi_o=0.5$ with an optimal value of $A_H=-1.07939$.

As opposed to this, it is discovered that the estimated scattering (Fourier) amplitude, A_S, in the square phase, S, for the negative value of Φ_o is the same as that of the corresponding positive value of Φ_o (Fig. 5[ii]). As a result, the contour plot of $\Phi_S(r)$ after accounting for the value of A_S shows the same pattern for positive Φ_o and the equivalent negative Φ_o. For instance, Fig. 5[ii] displays a contour plot of $\Phi_S(r)$ at $A=-7$, $B=1$, and $\Phi_o=-0.05$ with an optimum value of $A_S=1.24588$. It should be noticed that the contour plot of $\Phi_S(r)$ with optimal values of $A_S=1.24588$ and $A=-7$, $B=1$, and $\Phi_o=0.05$ is identical to the one before. Also, the contour map shows an indivisible square lattice formed by the regions with the lowest and highest electron densities. This is the core columns scattered on the square lattice in the alkyl chain matrix, or one might say that the alkyl chain columns are spread out on the square lattice in the core matrix.

In conclusion, we may state that the (D) phase, is the initial phase that occurs when value of Φ_o is low. The H_I phase, where columns of core are placed on the 2D-hexagonal lattice in the matrix of alkyl chains, is however brought about by an increase in the value of Φ_o. As Φ_o continues to rise in value, the S phase results. If the value of Φ_o is increased further, the phase changes into the H_{II} phase, which includes columns of alkyl chains arranged on a 2D hexagonal lattice in the matrix of the core. The (D) phase results from further increase in the value of Φ_o. Therefore, the current theoretical study stabilizes the different ordered phases in the following order: $disorder(D)$ - H_I - S - H_{II}

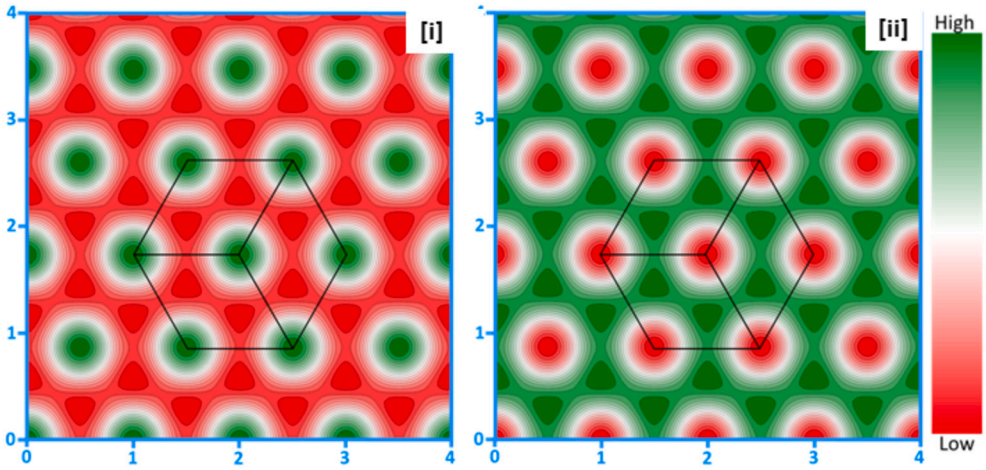

Fig. 6. [i] Displaying the contour plot of $\Phi_H(r)$ at $A=-7$, $B=1$, $\Phi_o=-0.5$ with optimal value of $A_H=1.07939$, where the only region that may display the 2D hexagonal lattice is that with the highest electron density. [ii] In the contour plot of $\Phi_H(r)$ at $A=-7$, $B=1$, and $\Phi_o=0.5$ with optimal value $A_H=-1.07939$, only region with the lowest electron density may exhibit the 2D hexagonal lattice. Scale is given in the unit of the lattice parameter. The hexagon in the black color is the conventional unit cell of the 2D hexagonal lattice. The conventional unit cell consists of three primitive unit cells.

- $disorder(D)$ as the average volume fraction difference, Φ_o, increases. Moreover, the above-described behavior of a discotic molecule with a rigid core and peripheral alkyl chain systems can be explained in terms of a gradual decrease in the spontaneous mean curvature of the rigid core-alkyl chain interface with increasing Φ_o, from being positive at low values of Φ_o to being negative for high values of Φ_o. One may also realize the following phase sequence by holding the value of Φ_o constant and increasing the value of the parameter A: S - H_I - $disorder(D)$ or S - H_{II} - $disorder(D)$. It should be emphasized that while the theory utilizes a fairly typical and simplified representation of the energy density, which is easy to deal with, the phase sequences that result from it are not the comprehensive but relatively ordinary. Because many of the isotropic interactions between the discotic molecules in the theory are included in the terms of the parameters A and B in their average and simplified forms; their detailed nature, such as the orientation of the molecule, tilt of the columns, directional interactions like hydrogen bonding, etc., are not included in their original form.

Additionally, by fitting the phase boundaries, the stability region of the ordered phases H_I, S, and H_{II} in the $A-\Phi_o$ plane may be estimated. The quadratic equation shown below is determined to best reflect the phase boundaries:

$$A = C\,\Phi_o^2 \tag{17}$$

Where C is the parameter and the corresponding symbols for the phase boundaries of $H-D$ and $S-D$ are C_H and C_S, respectively. These parameters' best-fit values were $C_H=-4.93$ & $C_S=-504.72$ for $B=1$ and $C_H=-24.23$ & $C_S=-2527.67$ for $B=5$, respectively. Let's use $Area_{HI}$, $Area_S$, & $Area_{HII}$ to represent the stability areas of the H_I, S, and H_{II} phases in the A - Φ_o plane, respectively. The following integration expression can be used to determine the necessary area:

$$Area_S = \int_{-A}^{0} \Phi_o\, dA = \int_{-A}^{0} \sqrt{\frac{A}{C_S}}\, dA \tag{18a}$$

$$Area_{HI} = \frac{1}{2}\left[\int_{-A}^{0} \sqrt{\frac{A}{C_H}}\, dA - \int_{-A}^{0} \sqrt{\frac{A}{C_S}}\, dA\right] \tag{18b}$$

$$Area_{HII} = \frac{1}{2}\left[\int_{-A}^{0} \sqrt{\frac{A}{C_H}}\, dA - \int_{-A}^{0} \sqrt{\frac{A}{C_S}}\, dA\right] \tag{18c}$$

Due to the fact that all these ordered phases turn off at $A=0$ and turn on for negative values of A, the upper and lower integration limits were determined to be 0 and $-A$, respectively. Using the values of C in equation (Eq. (18)), the stabilized areas are determined. The computed areas for $B=1$ are determined to be as follows: $Area_{HI}=0.1353\ A^{\frac{3}{2}}$, $Area_S=0.0297\ A^{\frac{3}{2}}$, & $Area_{HII}=0.1353\ A^{\frac{3}{2}}$ The stability area ratio is approximately: $Area_{HI}:Area_S:Area_{HII}=1:0.22:1$. Similar areas calculated for $B=5$ are found to be $Area_{HI}=0.0611\ A^{\frac{3}{2}}$, $Area_S=0.0133\ A^{\frac{3}{2}}$, & $Area_{HII}=0.0611\ A^{\frac{3}{2}}$. The stability area ratio is around $Area_{HI}:Area_S:Area_{HII}=1:0.22:1$. This demonstrates that the S phase occupies roughly 10% of the overall area of the ordered phase, whereas the H_I and H_{II} phases each occupy around 45% of the total ordered phase area.

A similar approach is used to study the stability of the body-centered cubic, hexagonal, and lamellar phases of the amphiphile-water system [27]. The theory, however, does not account for the intermediate phases, which include the bicontinuous cubic phase, ribbon phases, and mesh phases, which arise between the hexagonal and lamellar phases through a series of intermediary micelle shapes [28–31].

D. Goshe et al. employed a mean field model to describe the transition from columnar rectangular to columnar hexagonal phase of the discotic molecules, assuming that the molecules are bi-axial in both phases. With rising temperature, a rectangular-hexagonal-nematic-isotropic phase sequence is discovered for shorter members of a homologous series, however the nematic phase is omitted from the computed phase sequence for higher members [20].

Columnar hexagonal (H) phase is the most abundant phase of discotic molecules as observed experimentally [32,33]. There are several systems, both experimental and simulated ones, that show a hexagonal to square transition with varying aliphatic chain volume [34–36]. Melamine interacts with hydrogen-bonding complimentary substances having flexible long aliphatic chains in either a 3:1 or 2:1 stoichiometry resulting in columnar hexagonal, columnar rectangular, or columnar square phases. The phase sequence described above is remarkably close to what was seen in the current theoretical analysis [34]. A series of liquid-crystalline honeycombs are generated by a series of 5,5‴-diphenyl tetrathiophenes with polar glycerol groups at either end and two lateral flexible chains that surround polygonal prismatic cells and are filled by the lateral chains. A discontinuous shift from triangular to square honeycombs occurs with increasing chain length, which is quite comparable to our observations [35]. In order to investigate the columnar phases of tri- and tetra-block liquid crystalline bolaamphiphiles, dissipative particle dynamics (DPD) simulations were used. By changing the lateral arm lengths, the columnar phases of three asymmetric X-shaped bolaamphiphiles are investigated, including an unfrustrated

kagome phase with hexagonal and triangular columns and two frustrated phases with octagonal and square columns [36].

There are several different types of self-assembled structures that have been seen in surfactant-DNA complexes in aqueous solutions [37–39]. The cationic surfactant exhibits a range of columnar configurations, including square, hexagonal, and super-hexagonal, depending on the surfactant's chain length [37]. When the ratio of surfactant to DNA molecules is changed rather than the surfactant's chain length, the surfactant-DNA complexes also exhibit a similar phase behavior [38]. It's interesting to note that cationic liposome-nucleic acid complexes display lamellar, hexagonal, and inverted hexagonal structures [39].

Numerous discotic substances have been shown to undergo a columnar rectangular to columnar hexagonal transition as the temperature increases, partially supporting theoretical expectations [40,41]. However, experimentally, we could not see such a transition mediated by square phase. Moreover, the present theory also predicts a change from the square to the inverted hexagonal phase, which might occur if the peripheral links are sufficiently short.

4. Conclusions

The ordered phases, notably the square and 2D hexagonal phases, are stabilized by the current theoretical analysis. Moreover, the direct hexagonal and reverse hexagonal phases are identified in this work, with the phases occurring in the following order: $disorder(D)$ - H_I - S- H_{II} - $disorder(D)$ with rise in average volume fraction difference, Φ_o. Contrarily, the H_I and H_{II} phases each take up about 45% of the overall area of the ordered phase, while the stability area of the S phase is roughly 10% of the entire area of the ordered phase. The phase behavior described above can be explained by the progressive decline in the spontaneous mean curvature of the stiff core-alkyl chain interface in the discotic molecule with increasing Φ_o, which goes from being positive at low values of Φ_o to being negative for large values of Φ_o. The current theory does not, however, account for the other columnar phases of the discotic molecules. However, the free energy formalism employed in the current study only included a scalar order parameter; the vector order parameter is not included in the study, and as a result, the outcomes are not fully explicated. Moreover, the findings of this study should motivate additional investigation into innovative structure prediction and stabilization of the remaining columnar phases.

CRediT authorship contribution statement

Santosh Prasad Gupta: Conceptualization, Data curation, Funding acquisition, Visualization, Writing – original draft. **Mukesh Chandra Bos:** Conceptualization, Data curation. **Shallu Dhingra:** Conceptualization, Data curation. **Santanu Kumar Pal:** Conceptualization, Data curation, Funding acquisition, Visualization, Writing – review & editing.

Declaration of competing interest

There are no possible conflicts of interest to disclose with this article.

Data availability

No data was used for the research described in the article.

Acknowledgements

S. P. Gupta expresses gratitude to Patna University for providing infrastructural resources and assistance. S. P. Gupta expresses gratitude to SERB-TARE (TAR/2021/000146) for providing funds and the fellowship. S. K. Pal thanks SERB-TARE (TAR/2021/000146) for the financial support.

References

[1] Israelachvili, Intermolecular and Surface Forces, 2nd ed., Academic Press, London, 1991.
[2] B.R. Kaafarani, Discotic liquid crystals for opto-electronic applications, Chem. Mater. 23 (3) (2011) 378–396, https://doi.org/10.1021/cm102117c.
[3] S. Chandrasekhar, G.S. Ranganath, Discotic liquid crystals, Rep. Prog. Phys. 53 (1990) 57, https://doi.org/10.1088/0034-4885/53/1/002.
[4] T. Geelhaar, K. Griesar, B. Reckmann, 125 years of liquid crystals-a scientific revolution in the home, Angew. Chem., Int. Ed. 52 (2013) 8798–8809, https://doi.org/10.1002/anie.201301457.
[5] K. Arakawa, Liquid crystal display having positive and negative birefringent compensator films, US005189538A, 1993.
[6] H. Mori, Y. Ito, Liquid crystal display with compensators having minimum retardations in the inclined direction, US005189538A, 1998.
[7] N. Boden, J. Clements, B. Movaghar, Fluid sensing device using discotic liquid crystals, US006423272B1, 2002.
[8] W.P.S. Sergeyev, Y.H. Geerts, Discotic liquid crystals: a new generation of organic semiconductors, Chem. Soc. Rev. 36 (2007) 1902–1929, https://doi.org/10.1039/B417320C.
[9] W. Pisula, K. Mullen, in: J.W. Goodby, P.J. Collings, T. Kato, C. Tschierske, H.F. Gleeson, P. Raynes (Eds.), Handbook of Liquid Crystals, vol. 8, Wiley-VCH, Weinheim, 2002, pp. 627–674.
[10] S. Kumar, Self-organization of disc-like molecules: chemical aspects, Chem. Soc. Rev. 35 (2006) 83–109, https://doi.org/10.1039/B506619K.
[11] T. Shimogaki, S. Dei, K. Ohtab, A. Matsumoto, Columnar mesophases constructed by hierarchical self-organization of rod-like diacetylene molecules, J. Mater. Chem. 21 (2011) 10730–10737, https://doi.org/10.1039/C1JM10817D.
[12] C. Tschierske, Micro-segregation, molecular shape and molecular topology – partners for the design of liquid crystalline materials with complex mesophase morphologies, J. Mater. Chem. 11 (11) (2001) 2647–2671, https://doi.org/10.1039/B102914M.
[13] I. Bala, J. De, S.K. Pal, Functional discotic liquid crystals through molecular self-assembly: toward efficient charge transport systems, in: Nanostructure Science and Technology, 2021.
[14] S.T. Hyde, Interfacial architecture in surfactant-water mixtures: beyond spheres, cylinders and planes, Pure Appl. Chem. 64 (11) (1992) 1617–1622, https://doi.org/10.1351/pac199264111617.
[15] S.M. Gruner, Stability of lyotropic phases with curved interfaces, J. Phys. Chem. 93 (22) (1989) 7562–7570, https://doi.org/10.1021/j100359a011.
[16] S. Leibler, D. Andelman, Ordered and curved meso-structures in membranes and amphiphilic films, J. Phys. 48 (1987) 2013–2018, https://doi.org/10.1051/jphys:0198700480110201300.
[17] M.W. Matsen, Stabilizing new morphologies by blending homopolymer with block copolymer, Phys. Rev. Lett. 74 (1995) 4225–4228, https://doi.org/10.1103/PhysRevLett.74.4225.
[18] M.W. Matsen, Phase behavior of block copolymer/homopolymer blends, Macromolecules 28 (1995) 5765–5773, https://doi.org/10.1021/ma00121a011.
[19] M.W. Matsen, F.S. Bates, Unifying weak- and strong-segregation block copolymer theories, Macromolecules 29 (4) (1996) 1091–1098, https://doi.org/10.1021/ma951138i.
[20] D. Ghose, T.R. Bose, C.D. Mukherjee, M.K. Roy, M. Sana, A molecular mean field model for a rectangular to hexagonal phase transitionin discotic liquid crystals, Liq. Cryst. 173 (1989) 17–29, https://doi.org/10.1080/00268948908033364.
[21] J.-P. Carton, E. Dubois-Violettes, J. Prost, Orientational ordering in discotic columnar phases. a theoretical approach, Liq. Cryst. 7 (3) (1990) 305–314, https://doi.org/10.1080/02678299008033808.
[22] T. Coussaert, M. Baus, Density-functional theory of the columnar phase of discotic Gay–Berne molecules, J. Chem. Phys. 116 (2002) 7744–7751, https://doi.org/10.1063/1.1467340.
[23] T. Garel, S. Doniach, Phase transitions with spontaneous modulation-the dipolar Ising ferromagnet, Phys. Rev. B 26 (1982) 325–329, https://doi.org/10.1103/PhysRevB.26.325.
[24] D. Andelman, F. Broçhard, J.F. Joanny, Phase transitions in Langmuir monolayers of polar molecules, J. Chem. Phys. 86 (1987) 3673–3681, https://doi.org/10.1063/1.451970.
[25] I.W. Hamley, The Physics of Block Copolymers, Oxford University Press, New York, 1999.
[26] G. Gompper, M. Schick, Correlation between structural and interfacial properties of amphiphilic systems, Phys. Rev. Lett. 65 (1990) 1116–1119, https://doi.org/10.1103/PhysRevLett.65.1116.
[27] S.P. Gupta, A.K. Kaushal, N.K. Gaurav, S. Kumari, S. Kumari, P. Kumar, A theoretical study on the stability of the classical phases of surfactant-water systems in the temperature-concentration phase diagram, Mol. Cryst. Liq. Cryst. 731 (1) (2021) 88–104, https://doi.org/10.1080/15421406.2021.1969324.
[28] S.S. Funari, M.C. Holmes, G.J.T. Tiddy, Microscopy, x-ray diffraction, and nmr studies of lyotropic liquid crystal phases in the c22eo6/water system: a new intermediate phase, J. Phys. Chem. 96 (1992) 11029–11038, https://doi.org/10.1021/j100205a076.

[29] S.K. Ghosh, R. Ganapathy, R. Krishnaswamy, J. Bellare, V.A. Raghunathan, A.K. Sood, Structure of mesh phases in a cationic surfactant system with strongly bound counterions, Langmuir 23 (2007) 3606–3614, https://doi.org/10.1021/la0631466.
[30] S.P. Gupta, V.A. Raghunathan, Controlling the thermodynamic stability of intermediate phases in a cationic-amphiphile–water system with strongly binding counterions, Phys. Rev. E 88 (2013) 012503, https://doi.org/10.1103/PhysRevE.88.012503.
[31] S.P. Gupta, Investigation of ordered mesh phases using their detailed reconstructed electron density maps, J. Mol. Liq. 315 (2020) 113831, https://doi.org/10.1016/j.molliq.2020.113831.
[32] I. Bala, S.P. Gupta, S. Kumar, H. Singh, J. De, N. Sharma, K. Kailasam, Hydrogen-bond mediated columnar liquid crystalline assemblies of c3-symmetric heptazine derivatives at ambient temperature, Soft Matter 14 (2018) 6342–6352, https://doi.org/10.1039/C8SM00834E.
[33] S.P. Gupta, M. Gupta, S.K. Pal, Highly resolved morphology of room-temperature columnar liquid crystals derived from triphenylene and multialkynylbenzene using reconstructed electron density maps, ChemistrySelect 2 (21) (2017) 6070–6077, https://doi.org/10.1002/slct.201701117.
[34] L.-X. Guo, Y.-H. Liu, L. Wang, M. Wang, B.-P. Lin, H. Yang, Hydrogen-bonding induced melamine-core supramolecular discotic liquid crystals, J. Mater. Chem. C 5 (2017) 9165–9173, https://doi.org/10.1039/C7TC03059B.
[35] X. Cheng, H. Gao, X. Tan, X. Yang, M. Prehm, H. Ebert, C. Tschierske, Transition between triangular and square tiling patterns in liquid-crystalline honeycombs formed by tetrathiophene-based bolaamphiphiles, Chem. Sci. 4 (2013) 3317–3331, https://doi.org/10.1039/C3SC50664A.
[36] M.A. Bates, M. Walker, Computer simulation of the columnar phases of liquid crystalline bolaamphiphiles, Liq. Cryst. 38 (2011) 1749–1757, https://doi.org/10.1080/02678292.2011.631301.
[37] M. Thomas, A. Chowdhury, A.K. Majhi, V.A. Raghunathan, Columnar liquid crystalline phases of surfactant-dna complexes, Liq. Cryst. 49 (7–9) (2022) 1184–1193, https://doi.org/10.1080/02678292.2021.2008033.
[38] A.V. Radhakrishnan, S. Madhukar, A. Chowdhury, V.A. Raghunathan, Influence of micellar size on the structure of surfactant-DNA complexes, Phys. Rev. E 105 (6–1) (2022) 064504, https://doi.org/10.1103/PhysRevE.105.064504.
[39] C.R. Safinya, K.K. Ewert, C. Leal, Cationic liposome-nucleic acid complexes: liquid crystal phases with applications in gene therapy, Liq. Cryst. 38 (11–12) (2011) 1715–1723, https://doi.org/10.1080/02678292.2011.624364.
[40] B. Soberats, M. Yoshio, T. Ichikawa, X. Zeng, H. Ohno, G. Ungar, T. Kato, Ionic switch induced by a rectangular–hexagonal phase transition in benzenammonium columnar liquid crystals, J. Am. Chem. Soc. 137 (41) (2015) 13212–13215, https://doi.org/10.1021/jacs.5b09076.
[41] A.C. Ribeiro, B. Heinrich, C. Cruz, H.T. Nguyen, S. Diele, M.W. Schroder, D. Guillon, Rectangular to hexagonal columnar phase transition exhibited by a biforked mesogen, Eur. Phys. J. E 10 (2003) 143–151, https://doi.org/10.1140/epje/e2003-00018-9.